ELSEVIER

Applied Surface Science 106 (1996) 457–465

applied surface science

The effects of carrier transport on the photoluminescence of degenerate electron–hole plasma in GaAs epilayers

E. Poles [a], S.Y. Goldberg [a], B. Fainberg [a], D. Huppert [a,*], M.C. Hanna [b], Y. Rosenwaks [c]

[a] *Raymond and Beverly Sackler Faculty of Exact Sciences, School of Chemistry, Tel Aviv University, Ramat Aviv 69978, Israel*
[b] *National Renewable Energy Laboratory, Golden, CO 80401, USA*
[c] *Faculty of Engineering, Tel Aviv University, Ramat Aviv 69978, Israel*

Received 17 September 1995; accepted 31 December 1995

Abstract

Time resolved photoluminescence (TRPL) is employed to study photogenerated electron–hole plasma expansion under strong illumination conditions in thin GaAs epilayer. We have observed spectral dependencies similar to ones which are usually observed on carrier's cooling. However, in our case they are caused by the diffusion of the degenerate electron–hole plasma perpendicular to the crystal surface. We have studied the influence of the degenerated carrier transport on the luminescence characteristics of bulk samples, both experimentally and by simulations. We suggest using this method to measure the transport coefficients of both degenerate and hot excess carriers in semiconductor structures.

1. Introduction

During the last decade there has been considerable interest in photogenerated carrier dynamics in III–V semiconductors. Various issues such as hot carrier cooling [1], minority carrier lifetime [2], surface recombination velocity [3], and carrier injection across semiconductor–liquid interfaces [4] are of interest. Time resolved photoluminescence (TRPL) is a good method for characterizing the above processes. In a typical experiment a very short laser pulse (usually under 1 picosecond (ps) in duration) excites the semiconductor sample with a photon energy greater than the energy band-gap, creating hot carriers. The electrons and holes then start to lose energy and finally reach the lattice temperature.

In general, two stages of carrier relaxation can be defined [5]. The initial carrier distribution immediately after the monochromatic laser pulse is highly nonthermal due to energy and momentum selection rules for optical absorption. The first stage of carrier relaxation involves the evolution of the nonthermal distribution to a thermalized distribution, whereby the photogenerated carriers come to equilibrium with themselves, but not with the lattice. The resulting thermalized hot carrier plasma can be assigned an effective temperature characterizing its distribution (Fermi–Dirac or Maxwell–Boltzmann). This carrier temperature is generally much higher than

* Corresponding author. Tel.: +972-640-8903/7012; fax: +972-640-9293; e-mail: huppert@chemdc2.tau.ac.il.

PII S0169-4332(96)00413-8

the lattice temperature; also, the electrons and holes may equilibrate separately, leading to different temperatures for electron and hole distribution.

The initial thermalization process occurs in a typical time scale of a few hundred femtoseconds [5] through ultra-fast events such as inter-valley scattering and carrier–carrier scattering. The initial excess kinetic energy of the carriers is not lost during this process, but is simply re-distributed among all the charge carriers of the system. The second stage of carrier relaxation involves energy loss, and cooling of the thermalized hot carrier plasma to the lattice temperature. For plasma temperatures greater than 40 K, longitudinal optical (LO) phonon emission is the dominant energy loss mechanism. The characteristic time scale for this second stage of carrier cooling in bulk material is between 1–10 ps depending on the carrier density [6].

The generally accepted point of view in the literature, is that only hot carrier cooling processes are responsible for the spectral evolution of the nonequilibrium luminescence (see for example [7]). This issue has been revised by Bailey and Stanton in their pioneering work [8]. Using an ensemble Monte Carlo method coupled with a $\boldsymbol{k}\cdot\boldsymbol{p}$ calculation of the band structure, they showed that on a picosecond scale, carrier transport even in a thin, 0.5 μm GaAs epilayer perpendicular to the layer, significantly reduces the density at the surface. They compared their calculated luminescence with the experimental data [7] and showed that transport affects strongly the photoluminescence decay.

Unfortunately, due to the numerical character of their study [8], the diffusion transport role of various spectral components of the luminescence is not quite clear. One can imagine the following possible ways that transport influences luminescence.

First, the energy distribution of carriers may only be adequately described by electron temperature T_e below the threshold of the optical-phonon emission $\varepsilon = \hbar\Omega_0$ [9] (passive region $\varepsilon < \hbar\Omega_0$). Above the threshold (active region $\varepsilon > \hbar\Omega_0$), the distribution critically depends on the photon energy and the laser pumping level [9]. In such a case, the transport velocity depends on the carrier energy which is reflected in the luminescence spectrum.

The second possibility can be related to the degeneracy of electron–hole plasma in GaAs at high-levels of excitation. For the degenerate regime the character of the electron energy distribution critically depends on density (the position of Fermi-level). The transport process changes the density of the carriers, and hence strongly affects their energy distribution. As a consequence, the luminescence spectrum is strongly dependent on the laser intensity. Low energy states will be occupied almost for any carrier densities, and diffusion weakly influences their populations. In contrast, the diffusion strongly affects the high level populations.

In this study we explore the role of transport processes on the luminescence of GaAs epilayers. We compare TRPL decay curves measured at several energies both on a very thin (0.5 μm) GaAs sample (where diffusion is relatively unimportant) and on a 5 μm thick sample. We found very profound differences between the high energy (above the band gap) luminescence spectra of the thin and thick samples. We also carried out power dependence measurements of PL at various wavelength. We show that the data of all our experiments in GaAs epilayers are consistent with the mechanism of carrier diffusion of degenerate electron–hole plasma, which can be characterized by a definite carrier temperature T_e. Any assumptions concerning the violations of a carrier distribution, characterized by a definite temperature [9], are not needed.

2. Experimental

The GaAs/AlGaAs heterostructures were grown by atmospheric pressure metalorganic chemical vapour deposition (MOCVD) at 725°C on (100) GaAs substrates using the techniques described in [3]. For all samples, a 0.4 μm buffer layer of Zn-doped GaAs ($P = 7\times10^{17}$ cm^{-3}) was first grown, followed by the desired structure which was non-doped. The samples were double heterojunction (DH) structures that contained capping layers of non-doped $Al_xGa_{1-x}As$ ($x = 0.48$) on either side of a GaAs epilayer. For the results reported here, two samples with different thicknesses of the active GaAs layers of 0.5 μm (sample A) and 5 μm (sample B) were used. The outer and inner $Al_xGa_{1-x}As$ barrier layers were 0.15 μm thick.

Time-resolved photoluminescence was measured using the time correlated single-photon counting (TCSPC) technique [2,3]. As an excitation source, we used a cw mode-locked Nd:YAG-pumped dye laser (Coherent Nd:YAG Antares and a 702 dye laser) at 600 nm providing high repetition rate (< 1 MHz) short pulses (2 ps) (FWHM). The TCSPC detection system is based on a Hamamatsu 3809U photomultiplier, Tennelec 864 TAC, Tennelec 454 discriminator and a personal computer-based multi-channel analyzer (nucleus PCA-II). The overall instrument response at FWHM was about 40 ps. The laser repetition rate and spot size were adjusted to create an initial electron–hole density not higher than 5×10^{18} cm^{-3} per pulse, in order to avoid crystal heating and prevent surface damage. TRPL spectra were taken at 10 nm intervals with 10 nm spectral bandwidth.

3. Results

3.1. General

The time resolved photoluminescence at several energies $h\nu_{PL} > E_{gap_o}$ was measured for two GaAs samples A and B. The absorption depth of the laser excitation pulse is ~ 2000 Å. The carrier cooling and transport in the case of the thin crystal is completed within a time shorter than the instrument response of 40 ps. At that point in time, the carriers are evenly distributed across the GaAs epilayer. In the case of the thicker crystal (sample B), the diffusion lasts for several nanoseconds during which the carriers are evenly distributed across the 5 μm thick layer.

The TRPL decay curve of sample B can be divided into three main time regimes. The first period of up to 10 ps reflects mainly the cooling of the initial hot carrier distribution, and the fastest stage of the transport process. The second period, a few picoseconds to a nanosecond in duration is dominated by the transport of carriers from the initial Beer–Lambert distribution into the bulk. The third time domain, a few nanoseconds to a microsecond, is controlled mainly by the radiative and nonradiative bulk recombination processes.

3.2. Thin crystal photoluminescence

Fig. 1 shows the TRPL curves measured at several photon energies in the range 1.43–1.75 eV (870–710 nm) of the 0.5 μm thick GaAs sample. The luminescence time decay curves at energies above 1.52 eV can be divided into two main regimes. The first is characterized by a very fast decay limited by the instrument response function. This fast decay is attributed to the photogenerated hot carrier relaxation to the lattice temperature. The larger the photon energy, the larger the amplitude of this short decay component. The cooling process as described in the introduction is fast (a few picoseconds), as is usually the case in bulk III–V semiconductors. The second time region of the decay curves is much longer than the former and is controlled by the radiative and nonradiative bulk recombination processes [3].

3.3. Thick crystal photoluminescence

Fig. 2 shows the time resolved photoluminescence curves of the thick (5 μm) GaAs sample measured at selected wavelengths in the spectral range of 870–710 nm (1.43–1.75 eV). In contrast to the TRPL curves of sample A (the thin sample), the PL curves of the thick sample, shown in Fig. 2, exhibit a nonexponential decay with three components. We attribute this to the transport of carriers from the surface region into the bulk.

As can be seen from Fig. 2 the decay time of the transport component in the PL decay curves strongly depends on the PL photon energy. The larger the photon energy (shorter PL wavelength), the shorter the lifetime of the transport component. The observed dependence of the PL decay time on the PL wavelength is much stronger than expected from the wavelength dependence of the PL reabsorption alone, and thus should be due to additional reasons. The strong dependence of the PL shape on the PL photon energy is explained by the transport of degenerated electron–hole plasma perpendicular to the crystal surface, as described later in the theoretical section and in the discussion.

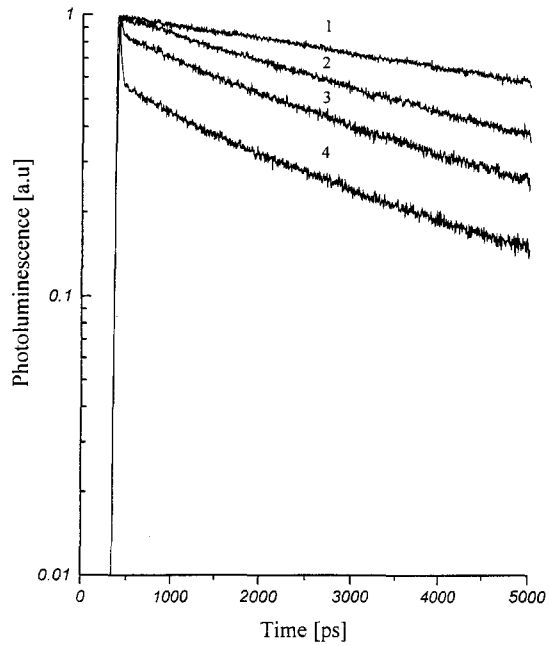

Fig. 1. Semilog plots of time resolved photoluminescence (PL) measured at various photon energies of 0.5 μm GaAs crystal. Curves 1, 2, 3 and 4 correspond to PL energy of: 1.43 eV, 1.49 eV, 1.57 eV, 1.65 eV, respectively.

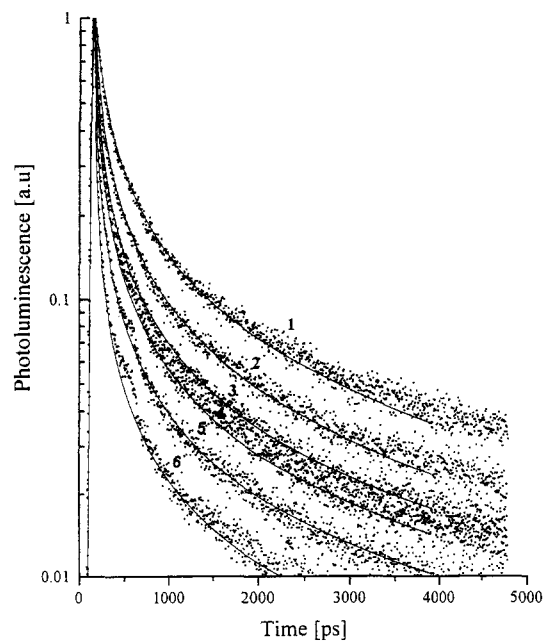

Fig. 2. Time resolved photoluminescence experimental data and computer simulations (solid line) of a thick 5 μm crystal. The PL photon energies: 1.49 eV, 1.53 eV, 1.57 eV, 1.61 eV, 1.65 eV, 1.70 eV are denoted as 1, 2, 3, 4, 5 and 6, respectively.

4. Theoretical consideration

Photoluminescence resulting from a direct radiative electron–hole recombination is commonly expressed by [10]:

$$I(\hbar\omega) \sim \omega^2(\hbar\omega - E_g)^{1/2} f_e f_h \tag{1}$$

where E_g is the band gap energy, and f_e and f_h are the electron and hole distribution functions, respectively. The distribution functions f_e and f_h differ in general from the equilibrium distribution since the carriers are generated by a nonthermal process (light pulse). However, for times relevant to our purposes they can be approximated ($t > 10$ ps) by thermal distributions which are equivalent to assigning a quasi-Fermi level to each type of carrier.

The electron and hole kinetic energies, E_e and E_h, measured relative to their respective band edges are related to the photon energy $\hbar\omega = E_e + E_h + E_g$.

We can write Eq. (1) in the following form:

$$I(\hbar\omega) \sim \omega^2(\hbar\omega - E_g)^{1/2} \left\{ \exp\left[\beta_e \left(\frac{m_h}{m_e + m_h}(\hbar\omega - E_g) - F_e \right) \right] + 1 \right\}^{-1} \times \left\{ \exp\left[\beta_h \left(\frac{m_e}{m_e + m_h}(\hbar\omega - E_g) - F_h \right) \right] + 1 \right\}^{-1} \tag{2}$$

here $\beta_c = 1/(kT_c)$, $\beta_h = 1/(kT_h)$, and m_e and m_h are the effective masses of electrons and holes, respectively; F_e and F_h are the corresponding quasi-Fermi levels, which are related to the local carrier densities n_c (c = e, h) by:

$$n_c = \frac{1}{(2\pi^3)^{1/2}} \frac{(m_c kT_c)^{3/2}}{\hbar^3} \mathscr{F}_{1/2}(\beta_c F_c) \tag{3}$$

where

$$\mathscr{F}_n(z) = \frac{1}{\Gamma(n+1)} \int_0^\infty \frac{x^n \, dx}{\exp(x - z) + 1}$$

is the nth order Fermi integral, and the quasi-Fermi levels are measured relative to their respective band edges.

The emission spectrum is obtained by integrating $I(\hbar\omega, x, t)$ taking into account reabsorption of the luminescence:

$$I(\hbar\omega, t) = \int_0^d I(\hbar\omega, x, t) \exp(-\alpha(\omega) x) \, dx, \tag{4}$$

where $\alpha(\omega)$ is the absorption coefficient at a specific emission energy, x is the optical path and d the crystal thickness.

The local carrier densities n_c ($n_e = n_h \equiv n$) satisfy the ambipolar diffusion equation [11]:

$$\frac{\partial n}{\partial t} = \vec{\nabla}(\mathscr{D}\vec{\nabla}n) + G + R \tag{5}$$

where G and R are the pair generation and recombination rates, respectively, and

$$\mathscr{D} = \mathscr{D}_e^0 \mathscr{D}_h^0 \frac{\mathscr{H}_{-1/2}^{1/2}(\beta_e F_e) + \mathscr{H}_{-1/2}^{1/2}(\beta_h F_h)}{\mathscr{D}_h^0 \mathscr{H}_0^{1/2}(\beta_e F_e) + \mathscr{D}_e^0 \mathscr{H}_0^{1/2}(\beta_h F_h)} \tag{6}$$

is the ambipolar diffusion coefficient, $\mathscr{D}_e^0 \sim T_e^{1/2}$ and $\mathscr{D}_h^0 \sim T_h^{1/2}$ are the low-density electron and hole diffusion constants, and $\mathscr{H}_k^m(\beta_c F_c) = \mathscr{F}_m(\beta_c F_c)/\mathscr{F}_k(\beta_c F_c)$.

The calculations show that for an electron density of $n \sim 3 \times 10^{18}$ cm^{-3} and $T = 300$ K the strong degeneracy condition [12] is satisfied for the electron system

$$\beta_e F_e = \frac{\beta_e \hbar^2 (3\pi^2 n_e)^{2/3}}{2m_e} \approx 4 \gg 1 \tag{7}$$

where we have used $m_e^* = 0.068 m_e$ for GaAs. For the heavy hole system, the corresponding parameter $\beta_h F_h < 1$, since the ratio $m_h^*/m_e^* \simeq 7.53$.

The electron and hole concentrations used in our experimental conditions, are about 10^{18} cm^{-3}. Therefore, as a first order approximation, we can consider the carrier system as degenerate for electrons, and as nondegenerate for the holes. In such a case, Eq. (2) becomes:

$$I(\hbar\omega, x, t) \sim \omega^2 (\hbar\omega - E_g)^{1/2} n_h \exp\left[- \frac{m_e}{m_e + m_h} \beta_h (\hbar\omega - E_g) \right] \times \left\{ \exp\left[\beta_e \left(\frac{m_h}{m_e + m_h} (\hbar\omega - E_g) - F_e \right) \right] + 1 \right\}^{-1} \tag{8}$$

In the degenerate case $\beta F_e > 1$ we have

$$F_e = \hbar^2 (3\pi^2 n_e)^{2/3} / (2m_e), \tag{9}$$

$$\mathscr{H}_0^{1/2}(\beta_e F_e) = \frac{4}{3\sqrt{\pi}} (\beta_e F_e)^{1/2}, \qquad \mathscr{H}_{-1/2}^{1/2}(\beta_e F_e) = \tfrac{2}{3} \beta_e F_e \tag{10}$$

and

$$\mathscr{D} \approx \mathscr{D}_e^0 \mathscr{D}_h^0 \frac{\frac{2}{3}\beta_e F_e + 1}{\mathscr{D}_h^0 (4/3\sqrt{\pi})(\beta_e F_e)^{1/2} + \mathscr{D}_e^0} \tag{11}$$

Since $F_e \sim n_e^{2/3}$ and n_e decreases with an increase of distance from the front surface, the ambipolar diffusion coefficient also decreases with distance.

$\eta(\omega, t) \equiv I(\omega, x = 0, t)/I(\omega, x = 0, t = 0)$ characterizes the decrease of the luminescence with time at a frequency ω from a very thin layer near the surface. From Eq. (8), we obtain:

$$\eta(\omega, t) = \frac{n_h(t)}{n_h(0)} \frac{\exp\{\beta_e [(m_h/(m_e + m_h))(\hbar\omega - E_g) - F_e(0)]\} + 1}{\exp\{\beta_e [(m_h/(m_e + m_h))(\hbar\omega - E_g) - F_e(t)]\} + 1} \tag{12}$$

Thus for the lower PL energies ('red frequencies'), satisfying the inequality [1]

$$\frac{m_h}{m_e + m_h} (\hbar\omega - E_g) - F_e(t) < 0 \tag{13}$$

(and consequently, $(m_h/(m_e + m_h))(\hbar\omega - E_g) - F_e(0) < 0$ since $F_e(0) > F_e(t)$)

$$\eta(\omega, t) = n_h(t)/n_h(0) \tag{14}$$

Hence the decrease of the 'red' PL frequencies is determined primarily by the decrease of the holes density n_h due to diffusion.

[1] We consider that $\beta_e |(m_h/(m_e + m_h))(\hbar\omega - E_g) - F_e(t)| \gg 1$.

For the 'blue' frequencies, satisfying the relation (see footnote 1): $(m_h/(m_e + m_h))(\hbar\omega - E_g) > F_e(0)$ and consequently

$$\frac{m_h}{m_e + m_h}(\hbar\omega - E_g) - F_e(t) > 0 \tag{15}$$

we obtain

$$\eta(\omega, t) \approx 2\frac{n_h(t)}{n_h(0)}\exp\left\{-\beta\left[\frac{m_h}{m_e + m_h}(\hbar\omega - E_g) - F_e(t)\right]\right\} \tag{16}$$

Eq. (16) shows an essentially faster decay of the 'blue' frequencies with respect to the 'red' ones (Eq. (14)). Thus, Eq. (16) qualitatively explains our experimental data shown in Fig. 2.

When the pump injection level increases (n increases) and/or the temperature decreases, the degeneracy of the hole system also becomes important, and one must use the general expression given by Eq. (2) for $I(\hbar\omega, x, t)$. For a strongly degenerated hole system and for 'red' PL frequencies satisfying both Eq. (13) and the condition

$$\frac{m_e}{m_e + m_h}(\hbar\omega - E_g) - F_h(t) < 0, \tag{17}$$

we obtain from Eq. (2) that $\eta(\omega, t) \approx$ constant, thus, the high laser injection level increases the degeneracy parameter and results in a slowing down of the red luminescence decay rate. The effect can be easily understood, since for a strongly degenerate gas the lowest states are occupied and the diffusion does not influence their populations. Such an effect explains our experimental data concerning the dependence of the red luminescence decay on the injection level.

5. Discussion

We have used the equations presented in Section 4 to simulate the PL experimental data of the 5 μm crystal shown in Fig. 2. The computer simulations are based on Eqs. (1)–(6). The initial total carrier density at $x = 0$, $t = 0$ was estimated to be $n_e(0, 0) = n_h(0, 0) = 3 \times 10^{18}$ cm^{-3}, based on the laser power, the spot size on the irradiated sample and the sample reflectivity. For simplicity, the initial hot electron carrier cooling process is assumed to be

$$T_e = T_L + \Delta T \exp(-t/\tau_c)$$

where T_e and T_L are the electron and lattice temperatures, respectively. ΔT is the initial ($t = 0$) temperature difference between the electron and the lattice, and $1/\tau_c$ is a constant characterizing the electron cooling time. The cooling time $\tau_c < 3$ ps as measured previously by several authors [1] is relatively short compared to the time resolution of our experiments ΔT was estimated from fitting the experimental data of the thin crystal (0.5 μm). The fast cooling process is seen in the TRPL data of the thin crystal shown in Fig. 1, as a fast decay limited practically by our instrument time response.

The dependence of the ambipolar diffusion constant on the carrier density is given in Eq. (4) where we assumed $T_e = T_h = 300$ K. Fig. 2 also shows the computer simulation fit of the experimental data (solid line). The hole diffusion constant used to fit the experimental photoluminescence is 4 cm^2/s.

The laser power dependence of the photoluminescence was discussed in the theoretical section. The power dependence of the PL at 870 nm (band edge) and at 750 nm (0.22 eV above the band gap) is shown in Fig. 3. At the edge luminescence (870 nm), the stronger the irradiation power the longer the decay time of the PL. The laser power dependence on the luminescence lifetime reverses when the PL energy is larger than the gap. At 750 nm the stronger the photoexcitation the shorter the PL decay time. The computer simulations of the laser

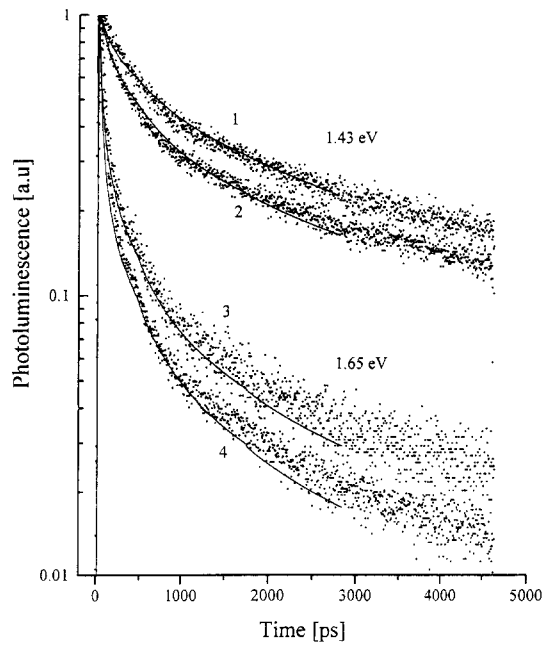

Fig. 3. Laser power dependence of time resolved photoluminescence curves. The two upper curves denoted 1 and 2, are measured at the band gap energy 1.43 eV, and the relative laser power is 4:1, correspondingly. The lower two PL curves 3, 4 are measured at 1.65 eV and the relative laser intensity is 10:1, respectively.

photo-carrier injection effect at high and low PL photon energies (see Fig. 3, solid line) are in good agreement with the experimental results.

6. Summary

We have used time-resolved photoluminescence to study photogenerated electron–hole plasma expansion under strong illumination conditions in thin GaAs epilayers. We have found profound differences between the high energy (above the band gap) luminescence spectra of thin (0.5 μm) and thick (5 μm) epilayers. As the degeneracy is determined by the carrier density, the TRPL spectrum is susceptible to carrier concentration changes. Thus, the TRPL spectrum is capable of measuring density changes due to diffusion. The photoluminescence spectrum is extremely sensitive to transport of degenerate electron–hole plasma, while in other methods [13–15] there are no qualitative differences between diffusions of degenerated and nondegenerated carriers. Hence we suggest that time-resolved photoluminescence can be a good method to measure the transport parameters of both degenerate and hot excess carriers in semiconductor structures.

References

[1] J. Shah, Solid State Electron. 32 (1989) 1051; Superlatt. Microstruct. 6 (1989) 293; Hot Carriers in Semiconductor Nanostructures (Academic Press, New York, 1992); C.L. Tang, F.W. Wises and D. Edelstein, Optoelectronics 1 (1986) 153.

[2] Y. Rosenwaks, L. Burstein, Y. Shapira and D. Huppert, J. Phys. Chem. 94 (1990) 6842; Appl. Phys. Lett. 57 (1990) 458; P. Besler-Podorowsky, D. Huppert, Y. Rosenwaks and Y. Shapira, J. Phys. Chem. 95 (1991) 4370.

[3] Y. Rosenwaks, Y. Shapira and D. Huppert, Phys. Rev. B 44 (1991) 13097; 45 (1992) 9108; M. Evenor, S. Gottesfield, Z. Harzion, D. Huppert and S.W. Feldberg, J. Phys. Chem. 88 (1984) 6213.

[4] Y. Rosenwaks, B.R. Thacker, R.K. Ahrenkiel and A.J. Nozik, J. Phys. Chem. 96 (1995) 10096.
[5] S.A. Lyon, J. Lumin. 35 (1986) 121.
[6] Z.Y. Xu and C.L. Tang, Appl. Phys. Lett. 44 (1984) 692; D.C. Edelstein, C.L. Tang and A.J. Nozik, Appl. Phys. Lett. 51 (1987) 48.
[7] D. Block, J. Shah and A.C. Gossard, Solid State Commun. 59 (1986) 527.
[8] D.W. Bailey and C.J. Stanton, Appl. Phys. Lett. 40 (1992) 880.
[9] S.E. Esipov and V.B. Levinson, Adv. Phys. 36 (1987) 331.
[10] A. Mooradian and H.Y. Fain, Phys. Rev. 148 (1966) 873.
[11] A. Othonos, H.M. van Driel, J.F. Ypung and P.J. Kelly, Phys. Rev. 43 (1991) 6682.
[12] A.I. Anselm, Introduction to the Theory of Semiconductors (Moscow, 1978) (in Russian).
[13] D.H. Auston and C.V. Shank, Phys. Rev. Lett. 32 (1974) 1120.
[14] C.A. Hoffman, K. Jarašiūnas, H.J. Gerritsan and A.V. Nurmikko, Appl. Phys. Lett. 33 (1978) 536.
[15] S.C. Moss, J. Lindle, H.J. Makey and A.L. Smirl, Appl. Phys. Lett. 39 (1981) 27.